Self-consistent electronic structure of lithium clusters

F. R. Redfern and R. C. Chaney
Department of Physics, University of Texas at Dallas, P.O. Box 830688, Richardson, Texas 75080-0688

P. G. Rudolf
Department of Physics, Trinity University, San Antonio, Texas 78284

(Received 4 April 1985)

The electronic structure of lithium clusters with 15, 27, and 59 atoms has been calculated self-consistently with use of the linear combination of atomic orbitals method. The results suggest that the conduction electrons in these clusters behave much like electrons in the spherical jellium-background model in that a similar shell-like structure is seen, albeit split by the crystal field. Friedel oscillations that appear in the conduction electron density are also much like those of jellium-sphere calculations. The crystal field removes the high degeneracy of the spherical symmetry, distributing the energy levels over the conduction band without destroying the shell-like structure. For clusters in the size range we have investigated, large energy gaps between shells should strongly influence cluster stability. Stability may also depend on crystal-field splitting to a lesser degree. In larger clusters the energy gaps between shells will become comparable to the crystal-field splitting and the shell-like structure will disappear. Mulliken population analysis and conduction-band widths indicate a trend towards bulk with increasing cluster size, although the electron density in the center of the largest cluster may not be entirely bulklike because of the penetration of Friedel oscillations.

I. INTRODUCTION

We have calculated self-consistently the electronic structure of isolated lithium clusters composed of 15, 27, and 59 atoms using the linear combination of atomic orbitals (LCAO) method and the local density approximation to the exchange potential of Kohn and Sham.[1] The clusters were constructed in body-centered-cubic (bcc) geometry by adding layers of rotationally equivalent lithium atoms (shells) around a central atom of lithium such that the clusters Li_{15}, Li_{27}, and Li_{59} consist of 3, 4, and 6 shells of atoms, respectively (counting the central atom as shell no. 1). The shell generating points are (0,0,0), (1,1,1), (2,0,0), (2,2,0), (3,1,1), and (2,2,2) in units of half a lattice constant. Lithium was chosen as a suitably simple material to work with since this study was primarily undertaken to develop self-consistent LCAO techniques for isolated clusters. The work presented here is an outgrowth of the cluster methods introduced by Chaney and Lin[2] and further developed by Rudolf and Chaney.[3,4]

The choice of cubic symmetry is one of computational convenience, since it seems unlikely that the structures we have adopted here will occur in significant amounts in bare metal clusters. For example, Knight *et al.*[5] report that the number of atoms in sodium clusters produced in a cluster beam is strongly governed by an inferred electronic shell structure, and Martins, Buttet, and Car[6] point out that highly symmetric clusters are likely to have a degenerate ground state and hence be subject to Jahn-Teller distortion. However, since our lithium clusters behave as jellium spheres subjected to a cubic crystal field, we believe the results we present in this paper embody some significance beyond the choice of cluster symmetry.

We chose the cluster lattice constant to be that of bulk lithium (6.597 bohrs), since we are interested in how well the central atom is screened from the surface perturbation, that is, how well it represents an atom in bulk lithium. This also motivated the choice of bcc structure for the clusters since this is the bulk structure of lithium. It is not entirely clear whether there will be net shrinkage or expansion in real lithium clusters due to lattice relaxation effects since both have been seen in calculations, depending on whether a bcc- or fcc-like (face-centered-cubic) structure is assumed.[7] Experimental evidence for copper and nickel clusters, however, suggests a decrease in interatomic spacing occurs as the number of atoms in a cluster decreases.[8]

The LCAO cluster calculation procedure we employ is basically that discussed by Rudolf and Chaney[4] taken to self-consistency for isolated clusters. As part of the procedure the electron density and the exchange potential are curve fit, and, with the use of an analytical basis set of Gaussians, the matrix elements of the Hamiltonian are computed exactly. Hence, the accuracy of the calculation depends only on computational considerations, namely the goodness of the curve fits and the completeness of the wave-function basis set, and on the local exchange-correlation approximation. In this regard our procedure differs from several other cluster techniques. The $X\alpha$ scattered-wave method[9] makes a muffin-tin approximation to the potential around the atomic cores and requires a constant potential between the muffin tins and a spherical potential enclosing the cluster. In the discrete variational method[10] the matrix elements are not calculated exactly but are approximations to the exact ones arising from the Rayleigh-Ritz variational procedure. Lee, Calla-

way, and Dhar[11] have presented an LCAO approach very similar to ours except that they perform a numerical integration to get the matrix elements for the local exchange-correlation potential. Hartree-Fock and configuration interaction techniques, which have been used for small clusters, are not very practical for systems as large as the ones we calculate because of the large number of four-centered integrals that need evaluation. Curve fitting the electron density and exchange potential substantially reduces the number of integrals while reducing the number of centers in the integrals to a maximum of three. However, performing these curve fits is the most involved part of our procedure, although we have developed techniques that have improved the quality of the fits and the time necessary to achieve them.

II. COMPUTATIONAL PROCEDURE

In atomic Hartree units our Hamiltonian is

$$H=-\tfrac{1}{2}\nabla^2-\sum_\nu \frac{Z}{|\mathbf{r}-\mathbf{R}_\nu|} + \int \frac{n(\mathbf{r}')}{|\mathbf{r}-\mathbf{r}'|}d\mathbf{r}' - \left[\frac{3n(\mathbf{r})}{\pi}\right]^{1/3}, \tag{1}$$

where the terms in order are the kinetic energy, the attractive potential of the nuclei at sites $\mathbf{R}_\nu$ with charge $Z=3$, the electron-electron repulsion of the electron density $n(\mathbf{r})$, and the Kohn-Sham exchange potential. The Kohn-Sham, one-electron equation to be solved for N electrons is

$$H\psi_1=\epsilon_i\psi_i$$

subject to (2)

$$n(\mathbf{r})=\sum_{i=1}^{N}|\psi_i(\mathbf{r})|^2 .$$

We expand the eigenfunctions ψ_i in terms of a basis set consisting of Gaussians with atomic symmetry centered on the atoms in the cluster. This basis set is transformed using group theory to a new one which block diagonalizes the Hamiltonian and overlap matrices that arise from the solution of the Kohn-Sham equation. This new basis set consists of linear combinations of the atomic-centered Gaussians and transforms according to the irreducible representations of the full octahedral group (O_h). If these basis functions are designated $\chi_j(\mathbf{r})$ for the jth basis function of some representation, then an eigenfunction in that representation can be expressed as

$$\psi_i(\mathbf{r})=\sum_i a_{ij}\chi_j(\mathbf{r}) , \tag{3}$$

where the coefficients a_{ij} are to be determined. Substituting into the Kohn-Sham equation and integrating yields the set of equations

$$\sum_j a_{ij}(\chi_k,H\chi_j)=\epsilon_i\sum_j a_{ij}(\chi_k,\chi_j) \tag{4}$$

for each irreducible representation. Matrix diagonalization techniques then give the eigenvectors a_{ij} and the eigenvalues ϵ_i. The Hamiltonian depends on the electron density and so the solution must be iterated to self-consistency. The electron density is found after each iteration by simply filling up the eigenstates with electrons until N electrons are accounted for.

Both the electron density and the exchange potential were fit using Gaussians and varying both the linear and nonlinear curve-fit parameters. For the electron density we placed spherically symmetric Gaussians [$B\exp(-Ar^2)$, with linear parameter B and nonlinear parameter A] on atomic and nonatomic ("floating") sites, the latter necessitated by the Friedel oscillations. The electron density and exchange potential were defined tabularly along a number of directions in the fundamental wedge, defined by $x\geq y\geq z$. We chose 334, 374, and 481 points in the fundamental wedge for the clusters Li_{15}, Li_{27}, and Li_{59}, respectively, in order to insure good resolution of electron density variations. This tabular density was fit by the method of least squares. It was advantageous to use floating Gaussians to help describe the exchange potential only in Li_{15}; however, a few nonspherically symmetric Gaussians of appropriate symmetry were included in the fits to the exchange potentials in Li_{27} and Li_{59}.

Curve fits of acceptable quality were attained with modest-sized basis sets. For example, an iteration-to-iteration least-squares error of 0.5% in the electron density with an electron number error of 0.05% was obtained by fitting Li_{59} with a total of 38 atom-centered and 11 floating Gaussians in the fundamental wedge, the floating Gaussians being distributed among 6 nonatomic sites. The same level of error was achieved with the smaller clusters. The exchange potential proved harder to fit. Least-squares errors ran about 1.6%, 1.3%, and 1.7% for Li_{15}, Li_{27}, and Li_{59}, respectively, using, for example, 49 atom-centered Gaussians in the fundamental wedge of Li_{59}. Much of the error was due to points well outside the clusters where the Kohn-Sham exchange potential falls off too rapidly with distance from the cluster and is therefore not accurate.[12] The balance of the error derives from points in the transition regions between the cores and the nearly homogeneous interstitial areas.

Our wave-function basis set was composed of the Gaussian-type orbitals of Eq. (9) in Chaney *et al.*,[13] and constituted 15 functions per atom. Attainment of self-consistency was judged by comparing the input and output electron densities. The same points used to calculate the curve fits were used to calculate the least-squares differences. In all three clusters input versus output least-squares differences of about 1.7% were the best attainable with reasonable effort. At this level of error the energy eigenvalues were virtually stationary.

III. RESULTS AND DISCUSSION

The densities of states (DOS) of the three lithium clusters are shown in Fig. 1, with the Fermi level marked by the vertical line. Discrete peaks are seen which, at least in the occupied part of the DOS, correspond to the electronic shells of a jellium sphere, a circumstance noted previ-

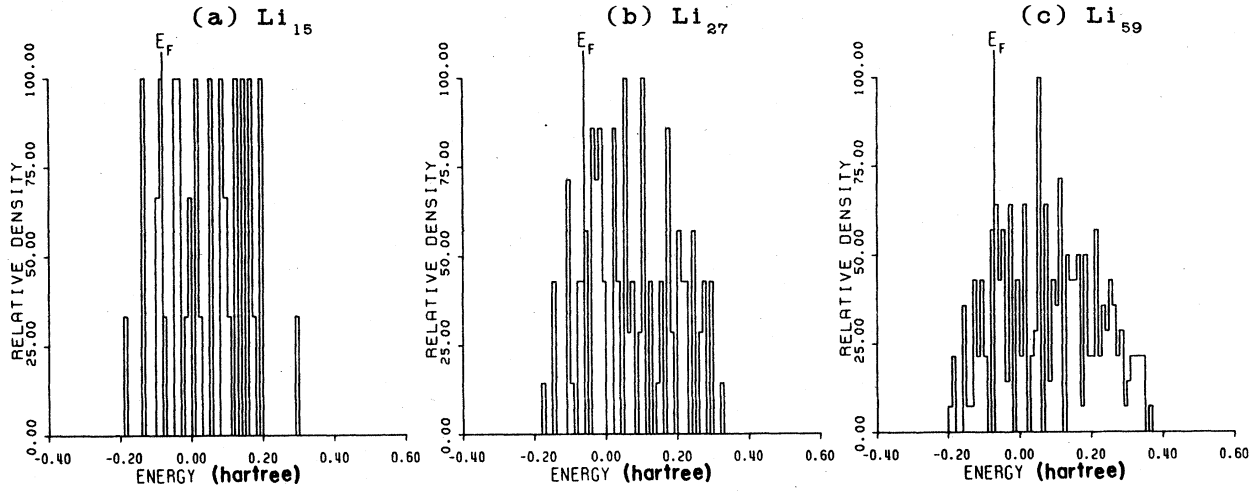

FIG. 1. Full DOS plots for lithium clusters.

ously by Geguzin for $X\alpha$, scattered-wave calculations.[14] The free-electron-like nature of the DOS is evidenced by the parabolic shape of the DOS, especially for Li_{59}. We list the Fermi level energies and conduction bandwidth data in Table I and compare them to the self-consistent bulk calculation of Ching and Callaway.[15] The method of their calculation was similar to ours in that an LCAO basis set of Gaussians in atomic symmetry and the Kohn-Sham exchange potential were used, only theirs was an extended crystal of bcc lithium. In Table I the conduction bandwidths of the clusters increase with cluster size and seem to approach the computed bulk value; the bandwidth for Li_{59} is 95% that of the bulk calculation. However, the Fermi energy and the energy at the bottom of the conduction band show no clear tendencies. This is a reflection of the surface energy of the clusters, which is not likely to vary uniformly with cluster size for small clusters that have not been allowed to relax. (Of course, the extended system of Ching and Callaway has no surface and therefore no surface contribution to the energy levels.)

In Fig. 2 we have attempted to separate the states in the interior of the clusters from the surface states by means of partial density of states (PDOS) plots. These PDOS plots were created by choosing only those single-electron eigenstates that overlap by more than a certain amount on specified cluster shells. The overlaps are calculated from projection operations as follows. The overlap onto basis function χ_j due to the eigenfunction ψ_i, is, using Eq. (3),

$$a_{ij}^*(\chi_j,\psi_i)=a_{ij}^*\sum_k a_{ik}(\chi_j,\chi_k)\,, \tag{5}$$

consistent with Mulliken population analysis.[16] These overlaps are sorted according to shell and energy yielding the PDOS. Exactly which atoms should be considered surface atoms is not obvious. Experience with the PDOS plots led us to choose shell 3 for Li_{15}, shell 4 for Li_{27}, and shells 5 and 6 for Li_{59}. The PDOS for these shells are narrower and are predominantly in a different energy range than the PDOS for the other shells. Obviously these "surface atoms" constitute a major percentage of the atoms in the clusters.

Common features can be seen in the PDOS plots. States with at least 60% overlap on the surface atoms [Figs. 2(a)–2(c)] are not occupied on Li_{15} and Li_{27} and few are occupied on Li_{59}. These "surface states" tend to avoid the energies that characterize the "interior states" [complementarily defined as those with at least 40% overlap on the interior atoms, Figs. 2(d)–2(f)] such that they fill a thin spot in the PDOS of the interior states. Since many of the states involved in this relationship are unoccupied and even unbound, the physical significance, if any, is not clear. However, the fact that the surface states tend not to be occupied may reflect the movement of electron density from surface to interior atoms with self-consistency. Were the atomic separations allowed to relax it is possible that occupied surface states would appear in greater numbers. The narrowing of the PDOS on the outer atoms compared to that of the full DOS is also evident in the figures. Narrow surface PDOS in metal clusters have been found by other investigators, including Salahub and Messmer for aluminum[17] and Delley *et al.* for copper.[18]

The electron density relative to bulk lithium is plotted in Fig. 3 in several radial directions not intersecting an atomic site for the clusters. The numbers appearing above the inverted triangles marking the radial distances of the shells are, from top to bottom, the coordination numbers (number of atomic nearest neighbors), the Mulliken popu-

TABLE I. Comparison of cluster energies with those of bulk (Ref. 15).

Property (eV)	Li_{15}	Li_{27}	Li_{59}	Bulk
Fermi energy	−2.30	−1.84	−2.15	−1.25
Energy at bottom of conduction band	−4.92	−4.69	−5.42	−4.70
Conduction-band width	2.62	2.85	3.27	3.45

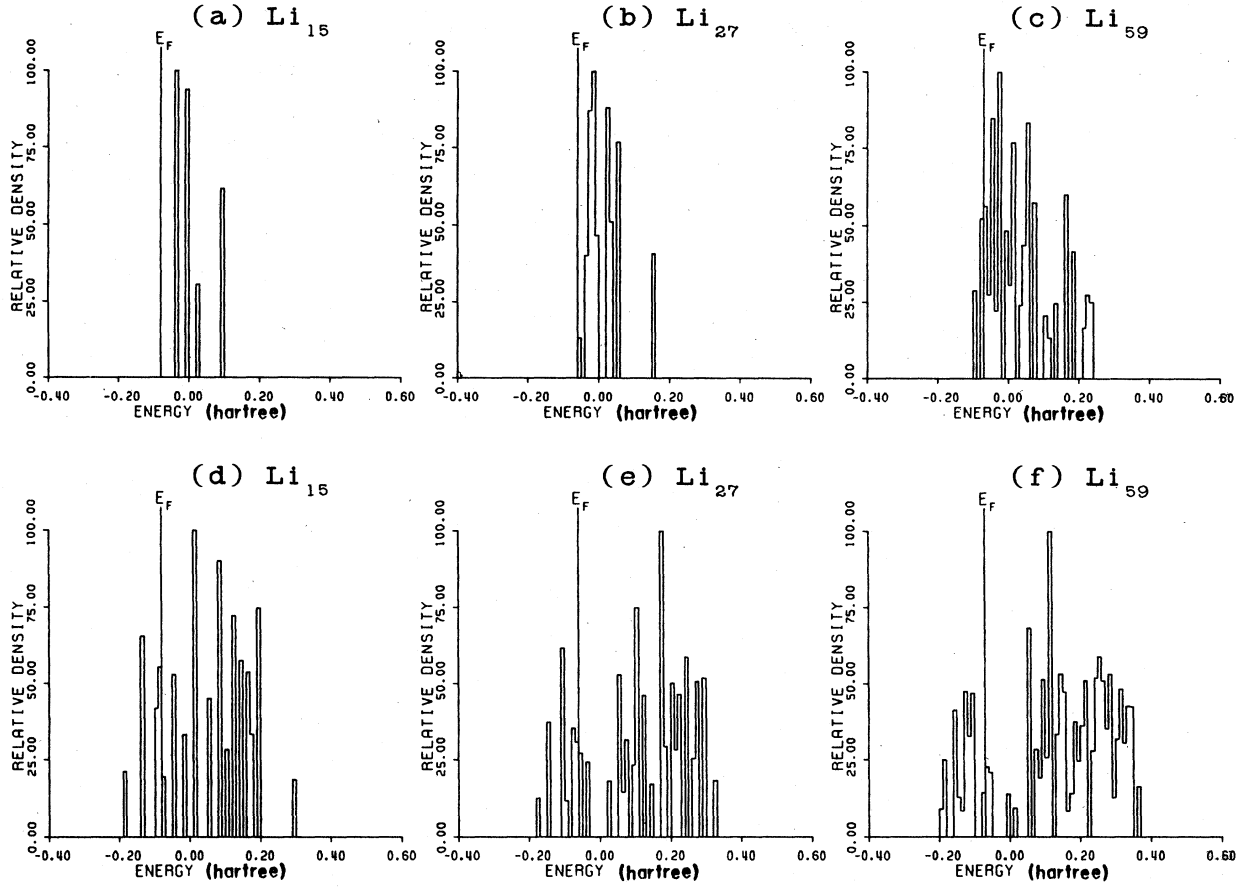

FIG. 2. Partial DOS plots for lithium clusters. 60% + overlap with surface atoms, (a)—(c); 40% + overlap with interior atoms, (d)—(f).

lations and the $1s$ core energies in units of eV for the atoms of each shell. The solid line in each plot delimits a sphere of homogeneous electron density corresponding to bulk lithium and containing an amount of charge equal to the number of conduction electrons in the cluster. The Mulliken populations reflect the movement of charge away from the surface atoms into the interior and provide some further justification for the choices of the surface atoms we made above. Prominent Friedel oscillations arising as a screening response to the surface perturbation appear in the electron density and are reflected in the Mulliken population numbers and to a lesser extent in the $1s$ core energies, which tend to be higher where the conduction electron density is thicker. It is interesting that the central atom in Li_{27} is characterized by a Mulliken population number of less than 3 (2.90), a consequence, at least in part, of the radial separation of the outer shell from the inner ones. Despite the slight departure from spherical symmetry, the electron density profiles of Fig. 3 are remarkably similar to those of similar-sized jellium spheres modeling sodium published recently by Ekardt.[19] Also evident in the plots is the moderation of electron density and Mulliken population variations toward the center of the largest cluster, indicating the development of bulklike characteristics.

Much of the structure of our full DOS plots (Fig. 1) can be understood by reference to Fig. 4, where the energy levels of the single-electron eigenstates are diagramed, labeled on the right by the irreducible representations of the O_h group to which they belong. On the left are the quantum numbers of a jellium sphere (see, e.g., Fig. 1 of Ref. 20), identified with the O_h levels by the effects of cubic-field splitting. The highest occupied state (Fermi level) is indicated and the accumulated occupancy at each level is given by the number at that level. The jellium-sphere electronic shell structure is clearly seen up to and just above the Fermi level for all three clusters. (Further up the energy scale the field-split jellium levels overlap and the shell structure disappears.) As cluster size increases, successive jellium shells fall below the Fermi level and telescope into the conduction band, increasing the DOS there. At some cluster size the field-split jellium shells near the Fermi level will begin to intermingle and lose their identity. (This occurs in the aluminum cluster calculation of Salahub and Messmer,[17] discussed below.) However, the jellium shells are still clearly visible in Li_{59}, even just above the Fermi level.

These observations are consonant with recent experimental findings of Knight *et al.*,[5] who produced a beam of sodium particles ranging in size from dimers to clusters

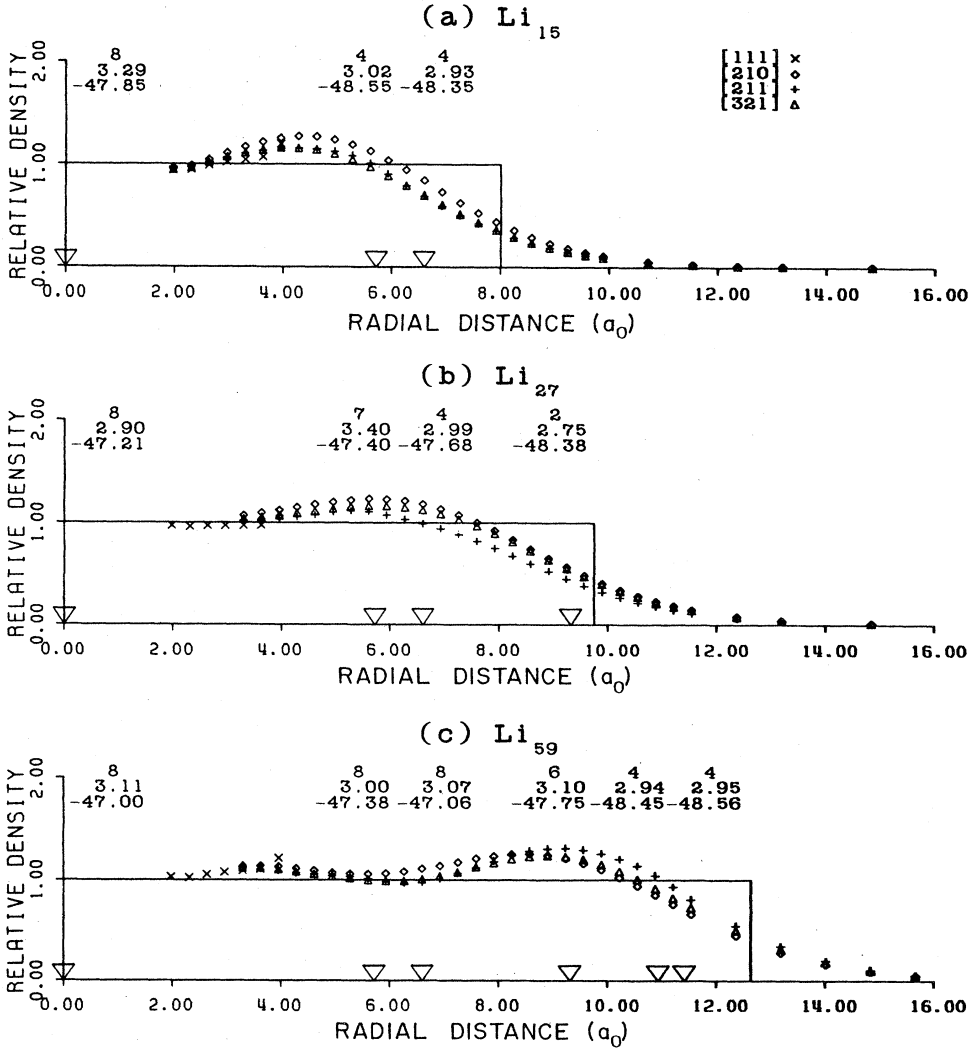

FIG. 3. Cluster electron density relative to bulk lithium plotted in several radial directions. The inverted triangles on the axis mark the radial positions of the atomic shells; the numbers above them are, from top to bottom, the coordination numbers, the Mulliken populations per atom and the 1s core energies in eV. The solid line in each plot delimits a sphere of uniform density corresponding to bulk lithium and containing the number of conduction electrons in the cluster.

of 100 atoms and measured the abundances of the different species by mass spectroscopy. Prominent peaks and/or steps in the mass spectrum [their Fig. 1(a)] were found at cluster sizes of 8, 20, 40, 58, and 92 atoms. They interpreted their results using a spherically symmetric potential based on the jellium sphere, observing that the prominent peaks/steps corresponded to filled jellium-sphere electron shells. Our results confirm this picture and may offer further contributions to understanding some of the structure in the mass spectrum.

If Li_{15}, Li_{27}, and Li_{59} are considered models for the smaller, medium and larger clusters, respectively, it is seen that the conspicuous cluster sizes of Knight *et al.*[5] correspond to cumulative occupation numbers below energy gaps at the top of jellium electronic shells. Note in particular the large gap between the $1p$-t_{1u} and $1d$-e_g levels (cumulative occupation number of 8) and between the $2s$-a_{1g} and $1f$-t_{2u} levels (cumulative occupation number of 20) in Fig. 4(a) for Li_{15}, then note the prominent peaks at cluster sizes 8 and 20 in Fig. 1(a) of Knight *et al.* Similar gaps associated with cumulative occupation numbers of 40, 58, and 92 are seen in Fig. 4(b) and 4(c). As explained by Knight *et al.*, a cluster size corresponding to the addition of an electron to a new jellium shell should be unfavored energetically because of the energy gaps between shells, whereas a closed shell cluster should be relatively favored. The presence of crystal-field splitting modifies this picture somewhat. For example, with increasing cluster size the energy gaps between jellium shells near the Fermi level will shrink to the same order as the field splitting and so the energy advantage for filled shells should disappear in the larger clusters. This effect is evi-

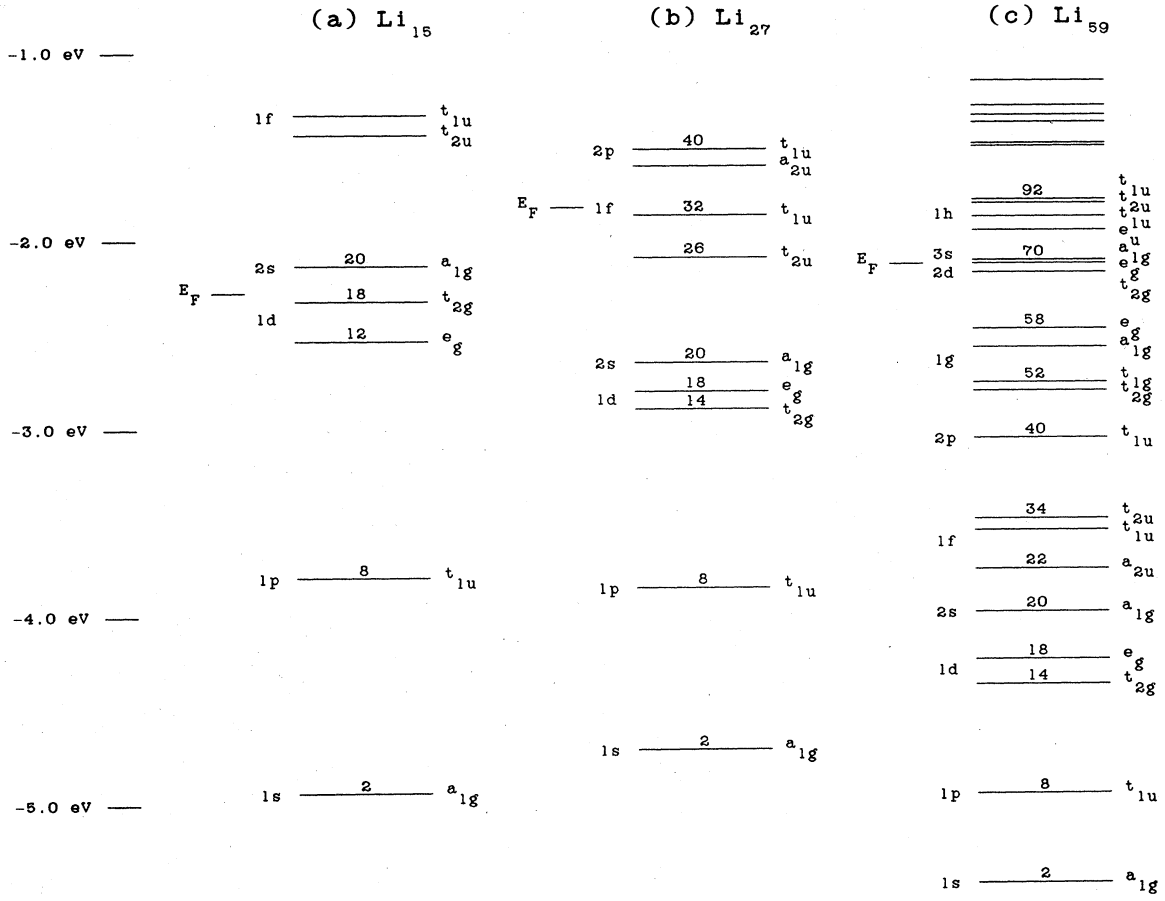

FIG. 4. Energy level diagram for lithium clusters. The numbers on the left of the levels identify the jellium electronic shells; those on the right the symmetry of the cubic group. The numbers above the energy levels are the cumulative occupation numbers.

dently seen in Fig. 1(a) of Knight *et al.*, where the mass spectrum structure gradually diminishes with increasing cluster size.

Few, if any, of the clusters seen in the mass spectrum of Knight *et al.* are likely to be in cubic symmetry, as we pointed out in the Introduction. As a result it can be expected that the actual crystal-field splitting will usually lead to energy levels less degenerate than those arising from a cubic field. In the absence of large exchange splitting, an asymmetric crystal field could result in a preference for clusters with an even number of electrons, since the crystal field cannot remove the spin degeneracy. An even-over-odd preference is noted by Knight *et al.*[5] in portions of their mass spectrum and also appears in the lithium cluster mass spectrum of Kimoto and Nishida.[21]

Realizing that the actual crystal-field splitting is unknown, it is still possible that some of the finer structure of the mass spectrum of Ref. 5 may be interpretable from our results. For example, we might relate the growth in the sizes of abundance peaks that occurs from clusters of 15 atoms to those of 20 atoms in the mass spectrum of Ref. 5 to the closeness of the $1d,2s$ field-split energy levels in the clusters. After these levels have come to be half-filled with electrons, it is reasonable that further growth in cluster size up to 20 atoms would be energetically favored since the $1d,2s$ complex must lower in energy with increasing positive cluster charge. Once these levels are filled, however, an energy gap inhibits the formation of a cluster with 21 electrons.

The interpretation of abundance peaks in terms of crystal-field splitting would have to be modified considerably were there large magnetic moments due to several unpaired electrons on small simple-metal clusters as implied by the spin-polarized, $X\alpha$, scattered-wave calculations of Geguzin[14] (sodium clusters in cubic symmetry) and Fripiat *et al.*[7] (lithium clusters in various geometries), since in this case exchange splitting might be as great as or greater than that due to the crystal field. However, the work of Ref. 6 implies that the preference for a high-spin ground state can be removed by the lowering of energy due to Jahn-Teller distortion. The effect of geometry on the magnetic properties of a cluster is illustrated by the two 13-atom clusters of Fripiat *et al.*: The 13-atom, cubo-octahedral lithium cluster shows little exchange splitting whereas the 13-atom icosahedron possesses five unpaired electrons. In support of low-spin ground states, no signals due to clusters with large magnetic moments were identified in Stern-Gerlach experiments performed

by Knight *et al.* on potassium clusters, and the results were interpreted to be consistent with the presence of one unpaired electron on clusters with an odd number of atoms and no unpaired electron on those with an even number.[22] Thus it may be that spin-unpolarized calculations of large symmetric clusters are better models of real ones than spin-polarized calculations of the same clusters which indicate possibly spurious magnetic properties. Because jellium-like behavior, which casts crystal-field splitting in the role of a perturbation, can be seen in simple-metal clusters calculated in various geometries,[7,14,17] spin-unpolarized calculations of large, highly symmetric clusters can be important in understanding real ones where the symmetries may be somewhat different. As pointed out by the authors of Ref. 6, who allowed their small sodium clusters to relax arbitrarily under the influence of Hellmann-Feynman forces, the electronic structure is not strongly dependent on the exact geometry.

Jellium electronic shells persist in the electronic structure of relatively large clusters. In the self-consistent, $X\alpha$, scattered-wave calculation of Salahub and Messmer[17] the shells are identifiable in an aluminum cluster as large as 43 atoms (129 conduction electrons) by comparing the DOS in their Fig. 2 with their Table II. However, the field-split jellium shells near the Fermi level of this cluster intermingle and begin to lose their identities, indicating the disappearance of the jellium electronic structure. In both the DOS plots of our lithium clusters and those of the aluminum clusters of Salahub and Messmer the Fermi level falls near a peak in the DOS. This is to be expected since the Fermi level will likely occur in the denser part of a field-split jellium shell. Since the electronic shells falls below the Fermi level and crowd into the conduction band with increasing cluster size, one must be careful in correlating cluster peaks to theoretical or experimental bulk peaks as was pointed out by Hintermann and Manninen in a similar observation.[20] The same caution may not apply as strongly to noble- and transition-metal clusters since *d*-band energy levels appear to aggregate in a relatively stable energy range as cluster size grows (examine, e.g., the results of Messmer *et al.*,[23] Yang *et al.*,[24] Rudolf and Chaney,[4] and Lee, Callaway, and Dhar[11]). One can even imagine that in a noble- or transition-metal cluster two electronic effects are active concurrently with increasing cluster size: delocalized, free-electron-like energy states crowd below the Fermi level, interacting and hybridizing with the more localized *d*-electron states, which accumulate in a fairly constant energy range.

How the electronic configuration of a metal cluster changes with growth in the number of atoms has been a topic of discussion.[25] The LCAO technique has the advantage of being able to supply Mulliken population numbers figuring in this question with little trouble since the LCAO basis set consists of atom-centered functions in atomic $(s,p,d,\ldots)$ symmetry.[16] To get these numbers, one performs projection operations as in Eq. (5) on occupied electron eigenfunctions and separates out the overlapping basis functions according to atomic symmetry. In what follows we refer to basis functions of *s* symmetry overlapping with basis functions of *s* symmetry as *s*-*s* overlaps, basis functions of *s* symmetry overlapping with those of *p* symmetry as *s*-*p* overlaps, and so forth. In Table II we list the gross and net atomic populations[16] for all atoms in the three clusters as well as occupancies per

TABLE II. Mulliken populations per atom sorted by shell and atomic symmetry for the three lithium clusters.

(a) Three-shell cluster

Overlap	1	2	3	Cluster
s-*s* (gross)	2.10	2.20	2.29	2.23
(net)	2.05	2.15	2.23	
s-*p* (gross)	0.43	0.40	0.37	0.39
(net)	0.00	0.13	0.02	
p-*p* (gross)	0.76	0.42	0.27	0.38
(net)	0.27	0.32	0.17	

(b) Four-shell cluster

Overlap	1	2	3	4	Cluster
s-*s* (gross)	2.00	2.16	2.16	2.32	2.22
(net)	2.09	2.08	2.09	2.25	
s-*p* (gross)	0.19	0.33	0.28	0.27	0.29
(net)	0.00	0.05	0.00	0.05	
p-*p* (gross)	0.71	0.91	0.55	0.16	0.49
(net)	0.20	0.59	0.23	0.05	

(c) Six-shell cluster

Overlap	1	2	3	4	5	6	Cluster
s-*s* (gross)	2.08	2.04	2.06	2.15	2.22	2.24	2.17
(net)	2.08	2.09	2.08	2.11	2.19	2.19	
s-*p* (gross)	−0.38	0.06	0.06	0.26	0.28	0.29	0.21
(net)	0.00	0.02	−0.01	−0.04	0.11	−0.01	
p-*p* (gross)	1.41	0.90	0.97	0.70	0.43	0.41	0.62
(net)	0.37	0.36	0.36	0.33	0.23	0.15	

atom for each cluster as a whole. Because of the delocalized nature of metallic eigenfunctions, the gross population for an atom, which in general includes cross terms from all the other atoms in the cluster, should not be considered definitive of local atomic symmetry. The central atom in each cluster is a special case of this since its net atomic population (which excludes cross terms by definition) for s-p overlap is necessarily zero by symmetry and hence s-p contributions to its gross atomic population will be entirely from cross terms. For instance, the odd value for the s-p overlap for the central atom of the six-shell cluster (-0.38) is due to strong negative overlaps with the outer two shells. However, we feel the gross atomic populations can be useful in spotting trends in clusters, especially when they are reflected in the net atomic populations.

For the clusters as a whole, a growing contribution of basis functions with p symmetry to the occupied eigenfunctions as cluster size increases is seen (Table II). Concurrently there is a relative decrease in s-p overlap terms. In bulk lithium it may be that $2s$ and $2p$ functions contribute nearly equally to the occupied bulk eigenstates, producing a ratio of p to s of about 3 to 1 in the conduction band since p atomic states are triply degenerate. From this point of view there is a trend toward bulk with increase in cluster size.

When the Mulliken populations of the individual atoms of each cluster are examined, a decrease in p-p and an increase in s-s overlap terms occurs as one proceeds outward from the central atom to the surface atoms. The s-p overlap terms are relatively larger for the two smaller clusters and much larger for the atoms near the surface of Li_{59} than for the interior atoms. These terms seem to be associated with the precipitous drop in electron density in the region of the outer shells. It is interesting that the occupied cross terms between atoms, which should reflect the bonding of the clusters,[16] consist predominantly of p-p and s-p overlaps of the longest-range basis functions. In fact these cross terms account for 49%, 54%, and 60% of the conduction-electron occupancies in Li_{15}, Li_{27}, and Li_{59}, respectively. The s-s overlap terms make small contributions by comparison. Since basis functions of p atomic symmetry seem to be strongly implicated in bonding in the clusters, the decrease in p character from the central to surface atoms noted above may be a function of the decreasing number of nearest neighbors, next-nearest neighbors, etc., in other words a bonding effect.

Because of the intense interest in impurities and point defects, how well the central atom in a cluster models an atom in the bulk material is a matter of concern.[4,20] Hintermann and Manninen[20] concluded from their work on self-consistent jellium spheres geared to the electron density of lithium that clusters must be rather large, on the order of 100 conduction electrons, to adequately describe bulk DOS, total energy and conduction bandwidth. Similar conclusions were reached by Ekardt[19] with regard to the ionization potentials and average electron energies of his self-consistent jellium spheres modeling sodium. However, much of the slow convergence of jellium sphere properties to those of infinite jellium can be ascribed to the high degeneracy of the energy levels,[19,20] and, as we have seen, the crystal field splits these and tends to distribute them over the energy range. In the case of impurities and point defects the major question concerns the environment with which these interact, not the approach to bulk of the cluster as a whole. Hintermann and Manninen, for example, showed that the induced electron density in a 22-electron jellium sphere with a central hydrogen atom was already a good approximation to that in infinite jellium. Also, Rudolf and Chaney[4] presented results for a hydrogen impurity at the center of a 38-atom nickel cluster implying that the hydrogen behaved approximately as it would in bulk. Although the electron density near the central atom in our 59-atom lithium cluster is rather bulk-like, the Friedel oscillations seem to penetrate all the way to its center (Fig. 3) just as in the larger jellium clusters of Ekardt. The question of modeling impurities in lithium and other metal clusters will likely have to be resolved by calculations introducing impurities into clusters with diverse numbers of atoms and observing the convergence of the properties of interest with cluster growth.

IV. CONCLUSIONS

Both experiment[5] and theory[19,20] have suggested that a free-electron metal cluster can be modeled in some respects by jellium spheres. The lithium clusters we have calculated indicate that such clusters are very much like jellium spheres in electronic structure and charge density. Jellium-sphere electron shells can easily be identified in lithium clusters of at least 59 conduction electrons and are seen in aluminum clusters[17] with over 100 conduction electrons. In addition, the density of the conduction electrons in our clusters is marked by prominent Friedel oscillations and quite similar to that calculated for jellium spheres.[19] It seems likely, in view of the work of Ref. 5, that the stability of free-electron metal clusters containing up to 100 conduction electrons is influenced to a large extent by the filling of jellium-sphere electron shells. The stability of clusters whose sizes fall between those corresponding to filled jellium shells may be partly due to how these shells are split by the crystal field. Crystal-field splitting tends to spread the electron energy levels over the energy range and therefore to modify the jelliumlike character of the clusters. As a result, it is possible that atomic clusters making bulklike hosts for impurities or defects can be smaller than is indicated in jellium-sphere studies.[20] Since the jellium electronic shells retain their identity in simple-metal clusters of up to 100 or more conduction electrons, the DOS will be dominated by such shell structure even in relatively large clusters.

The LCAO technique is useful in examining configuration and bonding effects in clusters using Mulliken analysis.[16] We find a large contribution of p atomic symmetry to the bonding of our lithium clusters, reflected perhaps in the decreasing p contribution to the Mulliken population numbers from the central atoms outward. An increasing p contribution with increasing cluster size may be a related phenomenon since the average atom in a large cluster has the opportunity to bond with more atoms than that in a small cluster. The directional nature of the s-p

cross terms in the electron density involves them in the exponential drop-off of the external density, and hence there is a relative decrease of these terms in larger clusters.

ACKNOWLEDGMENTS

This work was supported in part by the University of Texas at Dallas Organized Research Fund. Thanks are due to A. R. Redfern for suggestions on the manuscript.

[1]W. Kohn and L. J. Sham. Phys. Rev. **140**, A1133 (1965).
[2]R. C. Chaney and C. C. Lin, Phys. Rev. B **13**, 843 (1976).
[3]P. G. Rudolf, Ph.D. thesis, University of Texas at Dallas, 1980.
[4]P. G. Rudolf and R. C. Chaney, Phys. Rev. B **26**, 4378 (1982).
[5]W. D. Knight, K. Clemenger, W. A. de Heer, W. A. Saunders, M. Y. Chou, and M. L. Cohen, Phys. Rev. Lett. **52**, 2141 (1984).
[6]J. L. Martins, J. Buttet, and R. Car, Phys. Rev. B **31**, 1804 (1985).
[7]J. G. Fripiat, K. T. Chow, M. Boudart, J. B. Diamond, and K. H. Johnson, J. Mol. Catal. **1**, 59 (1975,76).
[8]G. Apai, J. F. Hamilton, J. Stohr, and A. Thompson, Phys. Rev. Lett. **43**, 1656 (1979).
[9]J. C. Slater and K. H. Johnson, Phys. Rev. B **5**, 844 (1972).
[10]E. J. Baerends, D. E. Ellis, and P. Ros, Chem. Phys. **2**, 41 (1973).
[11]K. Lee, J. Callaway, and S. Dhar, Phys. Rev. B **30**, 1724 (1984).
[12]J. P. Perdew, Chem. Phys. Lett. **64**, 127 (1979).
[13]R. C. Chaney, T. K. Tung, C. C. Lin, and E. E. Lafon, J. Chem. Phys. **52**, 361 (1970).
[14]I. I. Geguzin, Fiz. Tverd. Tela (Leningrad) **24**, 494 (1982) [Sov. Phys.—Solid State **24**, 278 (1982)].
[15]W. Y. Ching and J. Callaway, Phys. Rev. B **9**, 5115 (1974).
[16]R. S. Mulliken, J. Chem. Phys. **23**, 1833 (1955); **23**, 1841 (1955); **23**, 2338 (1955).
[17]D. R. Salahub and R. P. Messmer, Phys. Rev. B **16**, 2526 (1977).
[18]B. Delley, D. E. Ellis, A. J. Freeman, E. J. Baerends, and D. Post, Phys. Rev. B **27**, 2132 (1983).
[19]W. Ekardt, Phys. Rev. B **29**, 1558 (1984).
[20]A. Hintermann and M. Manninnen, Phys. Rev. B **27**, 7262 (1983).
[21]K. Kimoto and I. Nishida, J. Phys. Soc. Jpn. **42**, 2071 (1977).
[22]W. D. Knight *et al.*, Phys. Rev. Lett. **40**, 1324 (1978).
[23]R. P. Messmer, S. K. Knudson, K. H. Johnson, J. B. Diamond, and C. Y. Yang, Phys. Rev. B **13**, 1396 (1976).
[24]C. Y. Yang, K. H. Johnson, D. R. Salahub, J. Kaspar, and R. P. Messmer, Phys. Rev. B. **24**, 5673 (1981).
[25]M. G. Mason, Phys. Rev. B **27**, 748 (1983).